

# Hooking Together Sigmoidal Monomers into Supramolecular Polymers

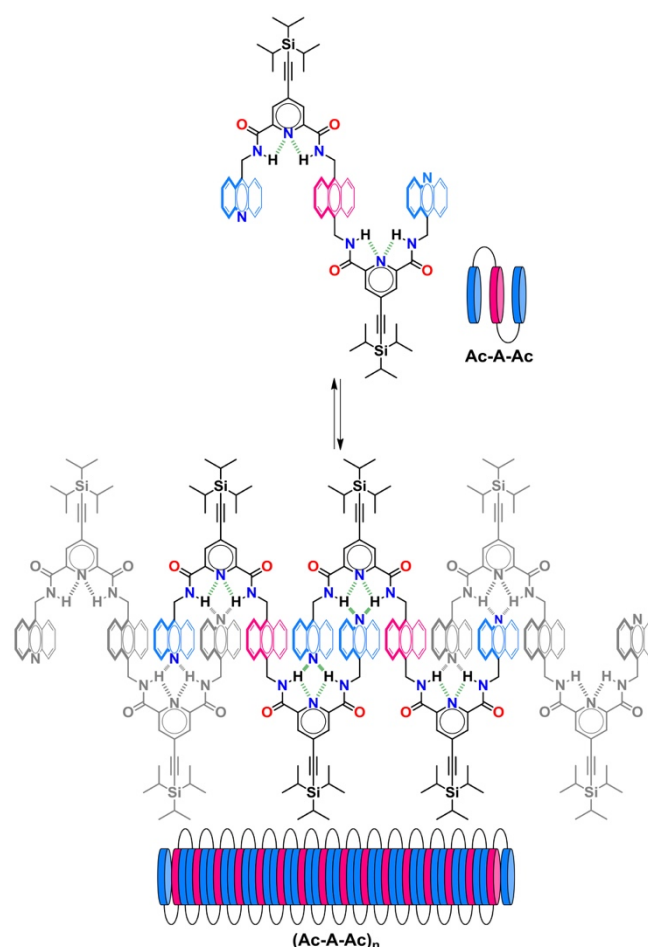
Marco Carini,<sup>[a]</sup> Mauro Marongiu,<sup>[a]</sup> Karol Strutyński,<sup>[b]</sup> Akinori Saeki,<sup>[c]</sup> Manuel Melle-Franco,<sup>[b]</sup> and Aurelio Mateo-Alonso<sup>\*[a][d]</sup>

**Abstract:** Supramolecular polymers have a lot of potential in the development of new materials because of their inherent recyclability and their self-healing and stimuli-responsive properties. Supramolecular conductive polymers are generally obtained by the assembly of individual disk-like  $\pi$ -conjugated molecules into columnar arrays that provide an optimal channel for electronic transport. We report a new approach to prepare supramolecular polymers by hooking together sigmoidal monomers into 1D arrays of  $\pi$ -stacked anthracene and acridine units, which give rise to micrometer-sized fibrils that show pseudoconductivities in line with other conducting materials. This approach paves the way for the design of new supramolecular polymers constituted by acene derivatives with enhanced excitonic and electronic transporting properties.

Supramolecular polymers play a pivotal role in materials science because of their inherent recyclability and their self-healing and stimuli-responsive properties.<sup>[1-2]</sup> Such properties are a direct consequence of their non-covalent nature and of the reversibility of the monomer to polymer equilibrium. Furthermore, the high directionality of non-covalent interactions, such as hydrogen bonds or  $\pi$ -stacking allows constructing ordered and shape-persistent nanometric and even micrometric polymeric assemblies with high precision by spontaneous self-assembly of molecular monomers.<sup>[3-4]</sup>

All the above-mentioned features make supramolecular polymers an ideal platform to develop materials for electronic applications, since efficient electronic transport is dominated by the precise spatial organization of organic semiconductors. For instance, lamellar  $\pi$ -stacking has been identified as an optimal molecular arrangement for electronic transport since it favours intermolecular electronic coupling.<sup>[5-17]</sup> Most supramolecular polymers for electronic applications involve the assembly of individual disk-like  $\pi$ -conjugated molecules (through hydrogen bonding, solvophobic,  $\pi$ -stacking and/or CT interactions) into columnar arrays in order to open an optimal channel for electronic transport.

**Scheme 1.** Synthesis and structure of supramolecular polymer (**Ac-A-Ac**)<sub>n</sub>.



Herein, we report a new family of supramolecular (**Ac-A-Ac**)<sub>n</sub> polymers that are obtained by hooking sigmoidal **Ac-A-Ac** monomers into a one-dimensional array of stacked anthracene (A) and acridine (Ac) units (Scheme 1). The **Ac-A-Ac** monomers are constituted by two external acridine units stitched to a central anthracene unit by 2,6-pyridinedicarboxamides. First, the **Ac-A-Ac** monomers fold into a sigmoidal hook-like conformation by intramolecular hydrogen bonds between the amides and the pyridinic nitrogen that gives rise to two adjacent antiparallel cavities of  $\sim 7$  Å. Then, the folded **Ac-A-Ac** monomer can be hooked into another folded **Ac-A-Ac** monomer by hydrogen bonds between the acridine nitrogen of one monomer and the amides of another monomer and by  $\pi$ -stacking. This monomer assembly mode leaves always two available cavities that promote the incorporation of additional monomers and therefore the formation of supramolecular (**Ac-A-Ac**)<sub>n</sub> polymers. In fact, the **Ac-A-Ac** monomers spontaneously self-assemble to provide

[a] Dr. M. Carini, M. Marongiu, Prof. Dr. A. Mateo-Alonso  
POLYMAT, University of the Basque Country UPV/EHU  
Avenida de Tolosa 72, 20018 Donostia-San Sebastian (Spain)  
E-mail: amateo@polymat.eu

[b] Prof. Dr. M. Melle-Franco and Dr. K. Strutyński  
CICECO - Aveiro Institute of Materials, Department of Chemistry,  
University of Aveiro  
3810-193 Aveiro, Portugal

[c] Prof. Dr. A. Saeki  
Department of Applied Chemistry  
Graduate School of Engineering Osaka University  
Suita, Osaka 565-0871 (Japan)

[d] Prof. Dr. A. Mateo-Alonso  
Ikerbasque, Basque Foundation for Science  
Bilbao (Spain)

micrometer long nanofibers with charge transporting properties similar to those of conducting polymers.

In addition to the self-assembling structural features described above, anthracene and acridine units were selected because of their excellent structural and electronic complementarity since they are constituted by three linearly fused rings and also because of their well-balanced properties in terms of charge transport, stability and solubility. Also, triisopropylsilyl (TIPS) groups have been introduced in the pyridine units to increase the solubility. To ensure that the **Ac-A-Ac** monomers are able to self-assemble into desired  $(\mathbf{Ac-A-Ac})_n$  polymers, a series of model experiments were carried out with **A-A** and **Ac-A** tweezer-like compounds (Figures 1 and 2) in order to understand the interactions between the different units and motifs. **A-A** has been prepared following a route described previously by some of us,<sup>[18]</sup> while all details of the synthesis and characterization of the **Ac-A** and **Ac-A-Ac** are given in the supporting information.

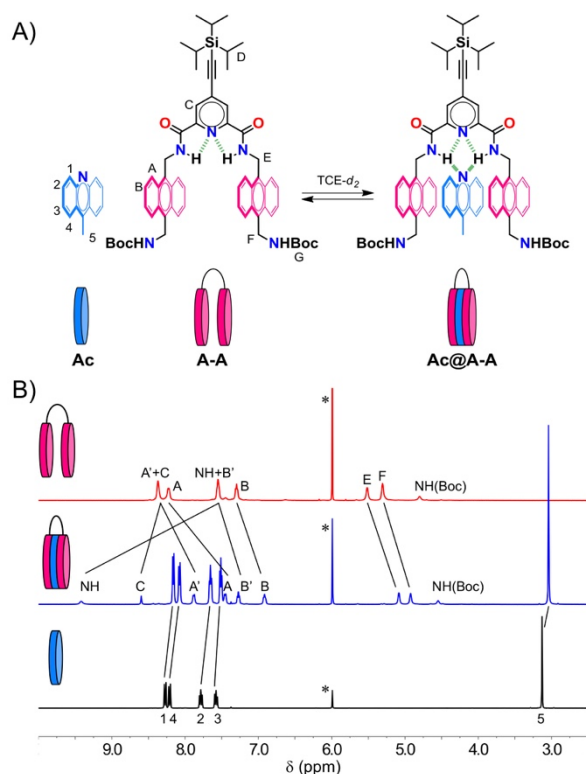


**Figure 1.** A) Scheme showing the assembly process between **A-A** and 9-methylacridine. B) <sup>1</sup>H-NMR of **A-A** (5 × 10<sup>-3</sup> M, 25 °C) in TCE-*d*<sub>2</sub> (red); <sup>1</sup>H-NMR of **A-A** (5 × 10<sup>-3</sup> M, 25 °C) with an excess (6 eq) of 9-methylacridine in TCE-*d*<sub>2</sub> (blue); <sup>1</sup>H-NMR of 9-methylacridine in TCE-*d*<sub>2</sub> (black). The asterisks indicate residual solvent peaks.

To ensure that acridines are able to self-assemble into the cavity of the folded **Ac-A-Ac** monomers, the supramolecular interaction between 9-methylacridine into the model **A-A** tweezers was studied (Figure 1). The NMR spectrum of a mixture of **A-A** in the presence of an excess of 9-methylacridine shows that the amide NH signals of **A-A** are deshielded in comparison to those of the

free **A-A**, which is consistent with the formation of hydrogen bonds with the nitrogen of acridine. Furthermore, the anthracene signals (A, A', B and B') and the 9-methylacridine signals (1, 2, 3 and 4) in the mixture are shielded in comparison to those of free **A-A** and free 9-methylacridine, respectively. These changes can be explained in terms of anisotropy because of the close proximity of the anthracene and acridine units as the result of  $\pi$ -stacking. NMR titration of **A-A** with increasing amounts of 9-methylacridine in 1,1,2,2-tetrachloroethane-*d*<sub>2</sub> (TCE-*d*<sub>2</sub>) (Figure S1) also evidenced similar changes in the NMR spectra consistent with the formation of the complex. From the titration experiments, an association constant ( $K_a$ ) of 1.4 × 10<sup>2</sup> M<sup>-1</sup> was estimated.<sup>[19-21]</sup>

One of the key steps in the formation of the  $(\mathbf{Ac-A-Ac})_n$  polymers rely on the formation of an assembly with four interacting anthracene and acridine units held together by two sets of intermolecular hydrogen bonds. Again, to ensure that the formation of such multimode assembly is possible, a model **Ac-A** tweezer that shows exactly the same self-recognition pattern as **Ac-A-Ac** but that upon self-assembly will evolve into the  $(\mathbf{Ac-A})_2$  dimer rather than into the  $(\mathbf{Ac-A-Ac})_n$  (Figure 2). To evaluate the homodimerisation of the **Ac-A**, <sup>1</sup>H NMRs in different solvents were recorded at different concentrations. The <sup>1</sup>H NMR spectrum recorded in dimethylsulfoxide-*d*<sub>6</sub> (DMSO-*d*<sub>6</sub>) show the individualised (undimerised) **Ac-A** since the aromatic signals (A, B, C, D, G and H) resonate all at the typical chemical shift values of anthracene and acridine derivatives (8.5–7.4 ppm) in this solvent. This is because of the high hydrogen bond basicity of DMSO disturbs the intermolecular hydrogen bond, favouring solvation rather than dimerization. The <sup>1</sup>H NMR spectrum of **Ac-A** recorded in TCE-*d*<sub>2</sub>, a solvent with a low hydrogen bond basicity that does not interfere with the hydrogen bonds, evidence the homodimerization of **Ac-A** into  $(\mathbf{Ac-A})_2$ . In fact, the NH signals resonate at chemical shifts consistent with the formation of hydrogen bonds (10.09 and 9.46 ppm). Moreover, the anthracene and acridine signals are broadened and appear strongly shielded (at 7.6–6.6 ppm) as an effect of anisotropy that support  $\pi$ -stacking. The ability of **Ac-A** to dimerise is also evidenced by matrix-assisted laser desorption ionization (coupled to a time-of-flight analyser) mass spectrometry (MALDI-TOF MS) that shows the  $[2M+Na]^+$  mass peak corresponding to  $(\mathbf{Ac-A})_2$  in the gas phase, besides the  $[M+H]^+$  and  $[M+Na]^+$  ions (Figure S2).

The homodimerization features in the <sup>1</sup>H NMR spectra are persistent upon dilution down to the NMR detection limit (~10<sup>-4</sup> M), which indicate that the dimerization constant ( $K_d$ ) is >10<sup>4</sup> (Figure S3). To overcome this,  $K_d$  was estimated by means UV-vis spectroscopy through dilution experiments from 10<sup>-4</sup> to 10<sup>-6</sup> M (Figure S4). By this method, a dimerization constant  $K_d = 8.56 \times 10^5$  M<sup>-1</sup> was estimated,<sup>[19-21]</sup> which is almost four orders of magnitude higher than the constant of the **Ac@A-A** complex.

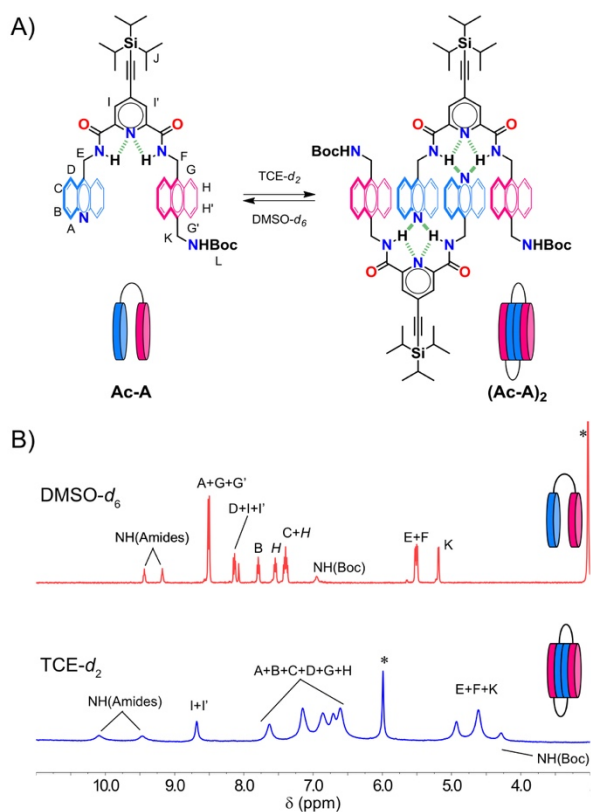


**Figure 2.** A) Scheme showing the dimerisation of **Ac-A**. B)  $^1\text{H-NMR}$  of **Ac-A** (80 °C) in  $\text{DMSO-}d_6$  (red) and of **Ac-A** (25 °C) in  $\text{TCE-}d_2$  (blue). The asterisks indicate residual solvent peaks.

The studies on the model compounds evidenced that the **Ac-A-Ac** monomer will be able to self-assemble in a similar fashion to **Ac-A** but providing two cavities that will enable the inclusion of additional monomers to provide **(Ac-A-Ac) $_n$**  (Scheme 1). In contrast to **Ac-A**, the **Ac-A-Ac** monomer was only found to be soluble during chromatographic purification from the crude mixture. Remarkably, after evaporating the solvent (chloroform) from the fractions containing **Ac-A-Ac**, a virtually insoluble material was obtained that could not be re-dissolved in any chlorinated solvent. This irreversible change of solubility of the **Ac-A-Ac** monomer is consistent with the formation of the **(Ac-A-Ac) $_n$**  supramolecular polymer upon the evaporation of the solvent. Definitive evidence of the formation of the **(Ac-A-Ac) $_n$**  polymer came from atomic force microscopy (AFM) and scanning electron microscopy (SEM). The AFM and SEM images of the **(Ac-A-Ac) $_n$**  dispersions in TCE revealed the presence of fibrils with a thickness of 20–40 nm that extend in length over several micrometers (Figures 3 and S5–S8). While the images of the deposited samples of **Ac-A** using the same conditions showed an unstructured film-like coverage of the surface with no evident morphology (Figure S9). This is consistent with the fact that **Ac-A** can only dimerise and not polymerise.

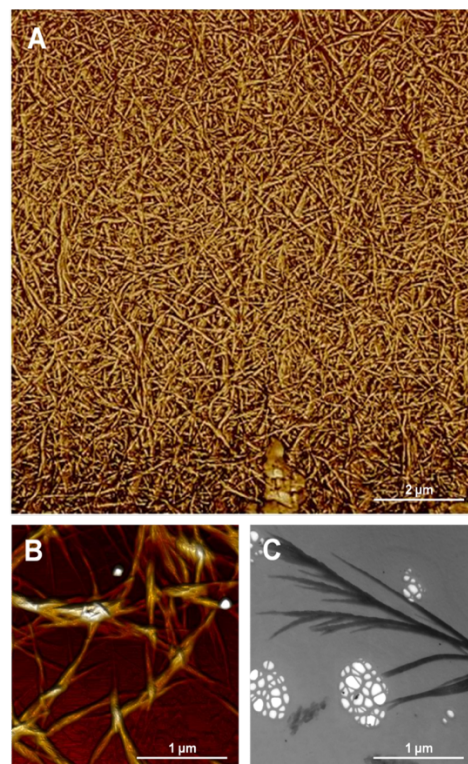


**Figure 3.** Morphology of the **(Ac-A-Ac) $_n$**  supramolecular polymer. A) AFM on mica 10x10  $\mu\text{m}$ . B) AFM on mica 2.5x2.5  $\mu\text{m}$ . C) SEM on holey carbon film coated copper grid 2.5x2.5  $\mu\text{m}$ .

The **(Ac-A-Ac) $_n$**  can be disassembled into smaller oligomers and even into monomers by increasing the temperature or by using solvents with a high hydrogen bond basicity. For instance, the **(Ac-A-Ac) $_n$**  polymer can be partially disassembled at high temperatures into smaller oligomers as illustrated by VT-NMR experiments in  $\text{TCE-}d_2$ , where the broad signals in the aromatic region split into partially resolved signals that resonate at the chemical shifts expected for the acridine and anthracene units (Figure S10). Also, **(Ac-A-Ac) $_n$**  polymer could be completely dissolved in trifluoroacetic acid (TFA) that strongly disturbs the hydrogen bonds and protonates the acridine nitrogen, as revealed by the  $^1\text{H NMR}$  in  $\text{TFA-}d_1$ , where structure of the disassembled **Ac-A-Ac** monomer was observed (Figure S11).

The intrinsic charge transport properties of the **(Ac-A-Ac) $_n$**  polymer were evaluated by means of flash-photolysis time-resolved microwave conductivity (FP-TRMC) measurements. This method measures directly the pseudoconductivity (defined as  $\phi\Sigma\mu$ , where  $\phi$  and  $\Sigma\mu$  are the photocarrier-generation yield and the sum of the mobilities of the generated charge carriers, respectively) without introducing electrodes. The  $\phi\Sigma\mu$  maxima can be considered the minimum mobility of the material since the  $\phi$  values are submultiples of the unit. A pseudoconductivity value  $\phi\Sigma\mu = 2.40 \times 10^{-4} \text{ cm}^2\text{V}^{-1}\text{s}^{-1}$  was estimated for the **(Ac-A-Ac) $_n$**  polymer from the resultant rise and decay profiles of transient conductivities (Figure 4A). These  $\phi\Sigma\mu$  values are in line with other conducting materials such as nanographenes,<sup>[22–23]</sup> stacked pseudorotaxanes,<sup>[24]</sup> peropyrene fibers,<sup>[25–26]</sup> and conjugated polymers.<sup>[27]</sup>



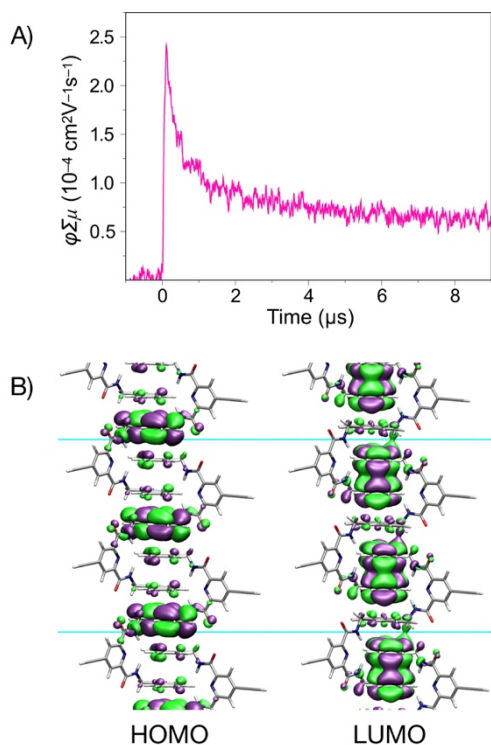


**Figure 4.** A) TRMC of  $(\text{Ac-A-Ac})_n$ . B) Frontier orbitals of  $(\text{Ac-A-Ac})_n$ .

To provide a picture of the electronic structure of **Ac-A-Ac**, theoretical calculations were carried out. For this, we first built a 1D crystal by replicating a suitably oriented molecule containing the aromatic core of **Ac-A-Ac**. Then, we explored configurational space by molecular dynamics and systematic minimizations with different 1D periodic lengths with a semiempirical tight binding model. The best minima found were then studied at the DFT GGA level while orbitals and corresponding energies were obtained with a hybrid Hamiltonian. The electronic structure and the orbitals of the frontier orbitals for the  $(\text{Ac-A-Ac})_n$ , in which the TIPS groups have been substituted by hydrogen, are qualitatively similar for studied cases (full details can be found in the supporting information). For each extra molecule in the periodic unit cell there is an extra nearly-degenerate HOMO and LUMO level. HOMO orbitals have consistently large densities on the anthracene moieties, while LUMO orbitals have consistently large densities on the two acridine neighbouring moieties (Figures 4B and S12). Remarkably, for all models, the electron densities of the frontier orbitals are spread throughout the stacked anthracene and acridine units, which act as channels for electronic transport.

To conclude, a new approach to prepare supramolecular polymers by hooking together sigmoidal **Ac-A-Ac** monomers into 1D arrays of stacked anthracene and acridine units has been reported. The **Ac-A-Ac** monomers are able to self-assemble by a combination of hydrogen bonds and  $\pi$ -stacking as demonstrated by a series of studies carried out on model compounds that show how **A-A** can complex acridine and **Ac-A** can dimerise, in a similar fashion as the **Ac-A-Ac** monomers. Furthermore, the **Ac-A-Ac** monomers have shown to form  $(\text{Ac-A-Ac})_n$  spontaneously giving rise to micrometer-sized fibrils that show pseudoconductivities in

line with other conducting materials. The approach reported here will pave the way for the preparation of supramolecular polymers constituted of acene derivatives, which combine the properties in electronic and excitonic transport and singlet fission of acenes with the recyclability and self-healing properties of supramolecular polymers.

## Acknowledgements

We are grateful to the Basque Science Foundation for Science (Ikerbasque), POLYMAT, the University of the Basque Country (Grupo de Investigación GIU17/054 and SGIker), Gobierno de España (Ministerio de Economía y Competitividad CTQ2016-77970-R), Gobierno Vasco (BERC program), Diputación Foral de Guipúzcoa (OF215/2016(ES)) and the Portuguese Foundation for Science and Technology (FCT), under the projects PTDC/FIS-NAN/4662/2014, IF/00894/2015, and FCT Ref. UID/CTM/50011/2019 for CICECO - Aveiro Institute of Materials. This project has been co-funded by the Erasmus+ programme of the European Union (contract 2018-1-IT02-KA103-047028). This project has received funding from the European Union's Horizon 2020 research and innovation programme under grant agreement No 664878 and from the European Research Council (ERC) under the European Union's Horizon 2020 research and innovation programme (grant agreement n° 722951). We thank Professor Pall Thodarson for help using the online tools for supramolecular chemistry research and analysis available at <http://supramolecular.org>

**Keywords:** supramolecular polymer •  $\pi$ -stacking • hydrogen bond • anthracene • acridine

- [1] T. Aida, E. W. Meijer, S. I. Stupp, *Science* **2012**, *335*, 813-817.
- [2] L. Yang, X. Tan, Z. Wang, X. Zhang, *Chem. Rev.* **2015**, *115*, 7196-7239.
- [3] D. D. Prabhu, K. Aratsu, Y. Kitamoto, H. Ouchi, T. Ohba, M. J. Hollamby, N. Shimizu, H. Takagi, R. Haruki, S.-i. Adachi, S. Yagai, *Science Adv.* **2018**, *4*.
- [4] N. Oya, T. Ikezaki, N. Yoshie, *Polymer Journal* **2013**, *45*, 955-961.
- [5] M. Mas-Torrent, C. Rovira, *Chem. Rev.* **2011**, *111*, 4833-4856.
- [6] C. Wang, H. Dong, W. Hu, Y. Liu, D. Zhu, *Chem. Rev.* **2012**, *112*, 2208-2267.
- [7] I. Yavuz, B. N. Martin, J. Park, K. N. Houk, *J. Am. Chem. Soc.* **2015**, *137*, 2856-2866.
- [8] R. Pfattner, S. T. Bromley, C. Rovira, M. Mas-Torrent, *Adv. Funct. Mater.* **2016**, *26*, 2256-2275.
- [9] C. Sutton, C. Risko, J.-L. Brédas, *Chem. Mater.* **2016**, *28*, 3-16.
- [10] J. P. Hill, W. Jin, A. Kosaka, T. Fukushima, H. Ichihara, T. Shimomura, K. Ito, T. Hashizume, N. Ishii, T. Aida, *Science* **2004**, *304*, 1481-1483.
- [11] K. Balakrishnan, A. Datar, R. Oitker, H. Chen, J. Zuo, L. Zang, *J. Am. Chem. Soc.* **2005**, *127*, 10496-10497.
- [12] F. Garcia, J. Buendia, S. Ghosh, A. Ajayaghosh, L. Sanchez, *Chem. Commun.* **2013**, *49*, 9278-9280.
- [13] B. W. Messmore, J. F. Hulvat, E. D. Sone, S. I. Stupp, *J. Am. Chem. Soc.* **2004**, *126*, 14452-14458.
- [14] F. S. Schoonbeek, J. H. van Esch, B. Wegewijs, D. B. A. Rep, M. P. de Haas, T. M. Klapwijk, R. M. Kellogg, B. L. Feringa, *Angew. Chem. Int. Ed. Engl.* **1999**, *38*, 1393-1397.
- [15] S. Xiao, J. Tang, T. Beetz, X. Guo, N. Tremblay, T. Siegrist, Y. Zhu, M. Steigerwald, C. Nuckolls, *J. Am. Chem. Soc.* **2006**, *128*, 10700-10701.
- [16] L. Zang, Y. Che, J. S. Moore, *Acc. Chem. Res.* **2008**, *41*, 1596-1608.
- [17] A. Jain, S. J. George, *Materials Today* **2015**, *18*, 206-214.
- [18] M. Carini, M. P. Ruiz, I. Usabiaga, J. A. Fernández, E. J. Cocinero, M. Melle-Franco, I. Díez-Pérez, A. Mateo-Alonso, *Nat. Commun.* **2017**, *8*, 15195.
- [19] <http://supramolecular.org>.

- 
- [20] D. Brynn Hibbert, P. Thordarson, *Chem. Commun.* **2016**, 52, 12792-12805.
- [21] P. Thordarson, *Chem. Soc. Rev.* **2011**, 40, 1305-1323.
- [22] D. Cortizo-Lacalle, J. P. Mora-Fuentes, K. Strutyński, A. Saeki, M. Melle-Franco, A. Mateo-Alonso, *Angew. Chem. Int. Ed.* **2018**, 57, 703-708.
- [23] J. P. Mora-Fuentes, A. Riaño, D. Cortizo-Lacalle, A. Saeki, M. Melle-Franco, A. Mateo-Alonso, *Angew. Chem. Int. Ed.* **2019**, 58, 552-556.
- [24] C. Gozalez, J. L. Zafra, A. Saeki, M. Melle-Franco, J. Casado, A. Mateo-Alonso, *Chem. Sci.* **2019**, 10, 2743-2749.
- [25] M. Martinez-Abadia, G. Antonicelli, A. Saeki, A. Mateo-Alonso, *Angew. Chem. Int. Ed.* **2018**, 57, 8209-8213.
- [26] M. Martinez-Abadia, G. Antonicelli, A. Saeki, M. Melle-Franco, A. Mateo-Alonso, *J. Org. Chem.* **2019**, 84, 3270-3274.
- [27] A. Saeki, Y. Koizumi, T. Aida, S. Seki, *Acc. Chem. Res.* **2012**, 45, 1193-1202.
-